WEP Warwick Evans Publishing

International Journal of Natural Resources and Environmental Studies

ISSN: 3006-2012 (Print), ISSN: 3006-0834 (Online) | Volume 8, Number 4, Year 2026
DOI: https://doi.org/10.62051/ijnres.v8n4.03
Journal homepage: https://wepub.org/index.php/IJNRES/index

Analysis of the Triggering Factors of Heavy Rainfall on Geological Disasters

Wenbin Zhao*

Institute of Resource and Environment, Henan Polytechnic University, Jiaozuo, Henan 454000, China

*Corresponding Author: Wenbin Zhao (212303020051@home.hpu.edu.cn)

ABSTRACT

Against the backdrop of global climate warming and intensified human activities, geological hazards triggered by heavy rainfall pose an increasingly prominent threat to the regional ecological environment as well as to human life and property. Taking Huixian City, Henan Province, as the study area, this paper systematically investigates the triggering factors and mechanisms of geological hazards induced by heavy rainfall through a combination of literature review, field sampling, and laboratory testing. First, the geological environmental conditions of Huixian City, including topography, stratigraphy and lithology, and meteorological-hydrological characteristics, were reviewed. Second, the physical and mechanical properties of typical silty clay in the study area were analyzed through direct shear tests and soil-water characteristic curve tests. The results show that the geological hazards in the area are mainly small- and medium-scale collapses, landslides, and debris flows, which are concentrated in low- to middle-mountainous and hilly areas and are highly consistent with heavy rainfall during the flood season (June to October) in both temporal and spatial distribution. The shear strength first increases and then decreases with increasing water content, cohesion reaches its peak at the optimum water content, and matric suction is significantly negatively correlated with water content. Finally, the core mechanism is clarified: heavy rainfall increases the water content of rock and soil masses, softens the rock-soil structure, and reduces the shear strength of the rock mass, thereby triggering geological hazards. The results of this study can provide a scientific basis and technical support for the monitoring, early warning, prevention, and control of geological hazards in Huixian City and other areas prone to similar geological hazards.

KEYWORDS

Heavy rainfall; Rainfall-induced geological hazards; Unsaturated soil; Soil-water characteristic curve; Shear strength.

1. INTRODUCTION

Geological hazards are destructive phenomena caused by the combined effects of natural environmental evolution and human disturbances. They not only result in casualties and property losses, but also cause irreversible damage to ecosystems, severely constraining regional sustainable development. Under global warming, extreme rainfall events occur more frequently. Heavy rainfall, as the most critical triggering factor for geological hazards, has become a key driver of collapses/rockfalls, landslides, debris flows, and related disasters, posing serious threats to life, property, and ecological stability in mountainous areas.

Henan Province is located in central China with complex and diverse geological conditions, and is one of the provinces with frequent geological hazards. According to statistics from the Henan Provincial Department of Natural Resources, since 2022 a total of 2,763 geological-hazard risk sites

have been identified, including 1,257 collapses, 1,021 landslides, 138 debris flows, 338 ground collapses, and 9 ground fissures. The hazard types are concentrated and the affected area is extensive. To address this challenge, Henan launched the construction of a flood-season meteorological forecasting and early-warning system for geological hazards as early as 2003, and completed the initial system in 2004 with expert review and acceptance, providing basic technical support for regional disaster prevention and control. Huixian City, a key area in northwestern Henan, lies on the southeastern flank of the Taihang Mountains. It features complex landforms, active structures, and a warm-temperate continental monsoon climate with concentrated precipitation and pronounced interannual variability, making it a critical region for hazard prevention in Henan. However, systematic studies on heavy-rainfall-induced hazards in Huixian City remain limited; existing results are insufficient to support precise risk reduction, and further research is urgently needed[1].

Extensive research has been conducted at home and abroad on the mechanisms of rain-induced disasters and their prevention and control. International studies began earlier [2] and have developed a mature framework of physical rainfall simulation[4], mechanistic modelling and threshold algorithms[2]: early work systematically compared four types of landslide-triggering rainfall thresholds (daily rainfall, initial rainfall, antecedent rainfall and antecedent soil moisture)[6]; subsequent field monitoring revealed the dynamic relationship between slope water content and rainfall infiltration[7]; and recent studies have integrated GIS and cellular-automata tools to achieve high-precision hazard assessment and prediction, establishing regionally adapted prevention and control systems[8]. Domestic research has focused on regional disaster characteristics, producing susceptibility zoning maps with ArcGIS[9], analysing in detail the initiation–transport–deposition processes of gully-type debris flows, and quantitatively correlating rainfall with landslides and rockfalls in mountainous and hilly areas[10]. Nevertheless, a systematic understanding of the micro-scale physical and chemical evolution of soil/rock structure and mineral composition during rainfall is still lacking, representing a key bottleneck hindering precise disaster prevention and control.

Based on the above background and remaining gaps, this study focuses on Huixian City and employs a combined approach of literature review, field sampling, and laboratory testing. The main tasks are: (i) compiling and analyzing geological-environment data (topography, lithology, meteorology and hydrology) to clarify the characteristics of hazard occurrence and evolution; (ii) summarizing local meteorological features and rainfall distribution patterns to explore the linkage between heavy rainfall and slope hazards; (iii) obtaining basic physical and mechanical parameters of soil samples through laboratory tests, establishing the SWCC, and analyzing the effect of water content on shear strength, thereby revealing the mechanism of slope-soil stability change under rainfall infiltration. This work aims to deepen the understanding of hazard genesis in the region, improve the theoretical framework of rainfall-induced disasters, and provide scientific evidence and technical support for monitoring, early warning, and prevention/mitigation in Huixian City and similar hazard-prone areas, promoting safe and orderly engineering construction and urban–rural development.

2. GEOLOGICAL BACKGROUND AND LABORATORY TESTS

2.1. Overview of the geological environment of the study area

2.1.1. Study the geological environment of the region

Huixian City is located in northwestern Henan Province (35°17′–35°50′ N, 113°20′–117°57′ E). Figure 1 shows its location at the border between Henan and Shanxi provinces. It borders Lingchuan County (Shanxi) to the west; is adjacent to Shanxi Province and Linzhou City to the north; neighbors Weihui City to the east; connects to Huojia County to the south; borders Xinxiang City to the southeast; and is adjacent to Xiuwu County to the southwest.

Fig 1. Location map of the study area

2.1.2. Topography and geomorphology

The study area is located at Shiziling of Jiufeng Mountain in western Huixian City, adjacent to the Taihang Mountains, with an elevation of about 1,732 m. The mountainous area covers 1,007 km², the hilly area 216 km², and the plain 784 km². The terrain is characterized by a transition belt of gentle slopes from northwest to southeast, generally showing a gradient from 2nd- to 3rd-order landforms. It includes deep mountain areas, low-mountain areas, hills, basins, piedmont plains, and low-lying zones, with the lowest elevation about 72 m.

2.1.3. Stratigraphy and lithology

Huixian City lies at the transition between the Taihang Mountains and the North China Plain. The strata exposed include the Archean, the Proterozoic (Sinian), the Paleozoic Cambrian and Ordovician, the Early Paleozoic Carboniferous and Permian, as well as the Tertiary and Quaternary. The Archean consists of a medium-grade regional metamorphic rock system, mainly forming valleys and hills. The dominant lithologies are biotite gneiss and plagioclase gneiss, with an exposed thickness of about 200–2,900 m, and the rock mass is relatively stable. In the central plains region, a belt of low to medium relief is formed with angular unconformity over the underlying Archean. Conglomerate layers a few centimeters to 10 cm thick are common at the contact. The lithology is relatively uniform, dominated by light yellow to purplish-red quartzite of moderate thickness, with horizontal/vertical bedding thickness of about 100–159.7 m. Cambrian strata of the Lower Paleozoic are important in the northwest and eastern parts of the area, with a total thickness exceeding 400 m, including the Lower (∈1), Middle (∈2), and Upper (∈3) series.

2.1.4. Meteorological and hydrological conditions

Huixian City is located at the junction of the Taihang Mountains and the North China Plain, near the boundary between the north subtropical and warm temperate zones, and has a warm-temperate continental monsoon climate. Affected by topography and elevation, monsoon effects are pronounced: windy springs, rainy summers, cool autumns, and winters with little snow. The climate can be divided into four sub-regions: (i) the northwestern cooler zone with short frost-free period and mean annual temperature below 12 °C; (ii) the Nancun Basin and shallow-mountain warm zone with mean annual temperature of 12–14 °C; (iii) the mountainous area with mean annual temperature of about 15 °C; and (iv) the plain area that is warm and humid with mean annual temperature around 14 °C. Based on statistics for 1971–2000, January is the coldest month (mean −0.6 °C) and July is the warmest (mean 27.1 °C). The extreme high temperature reached 45 °C on July 2, 1992, while the minimum temperature dropped to −18.3 °C on January 31, 1990. May has the longest sunshine duration (225.0 h). The mean annual precipitation is 589.1 mm, and the mean monthly precipitation is 182.3 mm. The mean annual relative humidity is 68%, with July and August averaging 79% and 80%, respectively.

As an important tributary of the Haihe River system, the rivers in Huixian include the Qi River, Baiquan River, Liudian Main Channel, Huangshui River, Shimen River, Yu River, Zhifanggou River and other tributaries. The South-to-North Water Diversion Project has been widely implemented in the western area. To meet flood control and irrigation needs, 19 small and medium reservoirs have been built. Reservoirs such as Huibaoquan, Shimen, Chenjiayuan and Sanjiaokou form a regulation system with a total length of about 86.5 km and can be operated for storage and release as needed.

2.2. Laboratory testing and analysis of typical soil parameters in the study area

2.2.1. Materials

Huixian City is located on the southeastern flank of the Taihang Mountains. The lithology is dominated by mudstone, sandstone and conglomerate, and the coarse-grained soil component is largely clay. The geological environment is complex and hazards occur frequently, making it a typical area for heavy-rainfall-induced geological hazards.

Considering sampling convenience and laboratory workload, together with the distribution of rock–soil masses in the study area, the sampling site was selected at a slope engineering site in Nanping Village, Shayaoxiang, Huixian City. Silty clay widely distributed in this area was chosen as the test material. The soil can represent the physical and mechanical characteristics of the main rock–soil types in the study area, providing reliable samples to investigate the influence of rainfall infiltration on stability. The physical properties are listed in Table 1.

Table 1 Physical property parameters of silty clay

Soil sample	Moisture content	Density	Plastic limit	Liquid limit	OMC
Silty clay	22.30%	$17.02 g/_{cm^3}$	24.50%	38.70%	25.1%

2.2.2. Analysis of soil-water characteristic test

In unsaturated soils, a water–air meniscus (often referred to as a “shrinkage membrane”) exists at the interface, creating surface tension. The air pressure in pores cannot be simply treated as equal to the water pressure, and is commonly higher. Therefore, the meniscus must sustain a larger pressure from the air phase, which is termed matric suction. For a given range of water contents, soil suction changes with water content and can be described by the soil–water characteristic curve (SWCC)[11]. At very low water contents, suction increases as water content decreases. Under the same water content, matric suction differs among soils and rocks. Because matric suction is determined jointly by meniscus curvature and interfacial (surface) tension, it cannot be simply calculated by S = Ua − Uw. Surface tension acts not only at the liquid surface, but also influences properties within the liquid body.

At the water–air interface, the interfacial strength decreases as temperature increases. A schematic of surface tension is shown in Fig. 2. Based on the calculation results, the pressure acting on the membrane surface can be obtained.

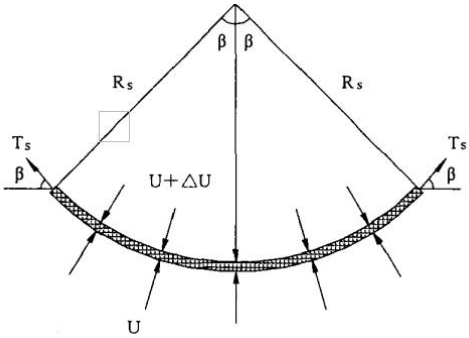

Fig 2. Pressure and surface tension at the water–air interface

$$\Delta u=\frac{T_S}{R_S} \tag{1}$$

where: R_S— radius of curvature of the meniscus; T_S — surface tension.

If the Laplace equation is used, Eq. (1) can be rewritten as:

$$\Delta u=\frac{2T_S}{R_S} \tag{2}$$

In unsaturated soils, pore-water pressure is usually lower than pore-air pressure. The meniscus sustains the pore-air pressure, and Eq. (2) can be modified as:

$$u_a-u_w=\frac{2T_s}{R_s} \tag{3}$$

According to Eq. (3), under saturated conditions the curvature of the interface tends to infinity and the suction drop becomes 0.

The SWCC test was conducted on silty clay collected from the Nanping Village slope in Shayaoxiang, Huixian City. Based on the principle that matric suction in unsaturated soils is generated by surface tension at the water–air interface (consistent with the Laplace equation), standard specimens with a dry density of 1.60 g/cm³ and a water content of 22.30% were prepared and allowed to equilibrate for 24 h. A combined pressure-plate and volume-membrane system was used. Measurements on unsaturated soil were performed using a ceramic plate and a pressurization system.

2.2.3. Direct shear test

To analyze the influence of water content on soil shear strength and to reveal the mechanical mechanism of heavy-rainfall-induced hazards, direct shear tests were carried out on silty clay from the Nanping Village slope in Shayaoxiang, Huixian City. Following the Standard for Soil Test Methods (GB/T 50123-2019), a YUC.IJZDY-1 single-box electric direct shear apparatus was used. Specimens with water contents of 21%, 23%, 25% and 28% were prepared, all with a dry density of 1.60 g/cm³. Three parallel specimens were set for each group. Normal stresses of 100 kPa, 200 kPa and 300 kPa were applied sequentially. After 5 min of stabilization, shearing was performed at a rate of 0.8 mm/min. Shear displacement and shear stress were recorded in real time until the shear-stress peak stabilized or the displacement reached 6 mm. After testing, outliers were removed and the Coulomb strength envelope was fitted linearly to determine cohesion (c) and internal friction angle (φ). Instrument calibration, specimen preparation and parallel testing were strictly controlled to ensure data reliability. The shear strength equation is as follows:

$$\tau=\sigma \tan \varphi +c \tag{4}$$

where: τ— shear strength of rock/soil, MPa; σ— normal stress on the shear plane, MPa; φ— internal friction angle; c— cohesion, MPa.

3. RESULTS AND DISCUSSION

3.1. Basic characteristics of geological hazards in Huixian mountainous areas

3.1.1. Spatial distribution of geological hazards in Huixian

Huixian is located on the southeastern flank of the Taihang Mountains. Geological environmental factors and human activities have a pronounced impact, making it a hazard-prone area in Henan Province. Various hazard types occur here, with collapses/rockfalls, landslides and debris flows being the most common. The distribution shows strong regionality and is influenced by topography/geomorphology, geological structure and human activities. Collapses, landslides and debris flows [7] are mainly distributed in the low–middle mountains to the west and north of the city and the hilly areas in the east and northeast. In the western and northern mountains, collapses are

mainly distributed in towns such as Bibi (Baibi) near the Baoquan Reservoir, Shangbali (Songshuping–Hesian'an No. 1), Sanjiaokou–Shayao, and areas such as Hankou (Huangshui Township) and Paishitou Township. Typical landslides include the Tixi slope landslide at Shuimo Village (Shayao Township), the Xiliansi landslide west of Songshuping Village (Shangbali Town), and the Guishan landslide near the Baoshan (Baoquan) Reservoir (Bibi Town). Debris flows mainly form in mountainous and hilly areas, and may also occur in some plains. Typical cases include Pingyanggou debris flow at Hesian'an (Shangbali Town), Zhuangwagou debris flow at Guoliang Village (Shayao Township), and Shangpinggou debris flow at Yanghesi (Shangbali Town). As shown in Fig. 3, 93 hazard sites were identified: 36 collapses (39%), 26 landslides (28%), and 31 debris flows (33%).

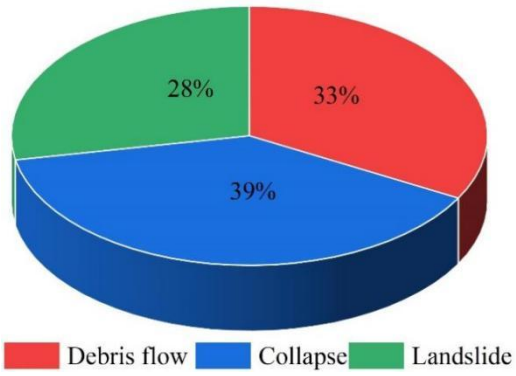

Fig 3. Statistics of geological hazard types

Statistical results of geological hazards by township are shown in Fig. 4. According to the Basic Requirements for Geological Hazard Investigation and Zoning at the county (city) level, hazards were classified by scale: there are 4 medium-scale collapses and 32 small-scale collapses; landslides include 3 large, 14 medium and 9 small events; and debris flows include 3 medium and 28 small events. These results indicate that the dominant hazards in Huixian are small- to medium-scale geological hazards.

According to the *Guidelines for Building a Mass-Monitoring and Mass-Prevention System for Geological Hazards* (Ministry of Land and Resources, 2005), the classification criteria for hazard severity and risk levels are as follows:

General: economic loss ≤ 5 million CNY and affected population ≤ 100; Relatively major: loss > 5 million CNY and < 50 million CNY, affected population 100-500; Severe: affected population > 500 and threatened population ≤ 1,000, with losses of 50-100 million CNY; Extra-severe: threatened population > 1,000, with property losses > 1 billion CNY.

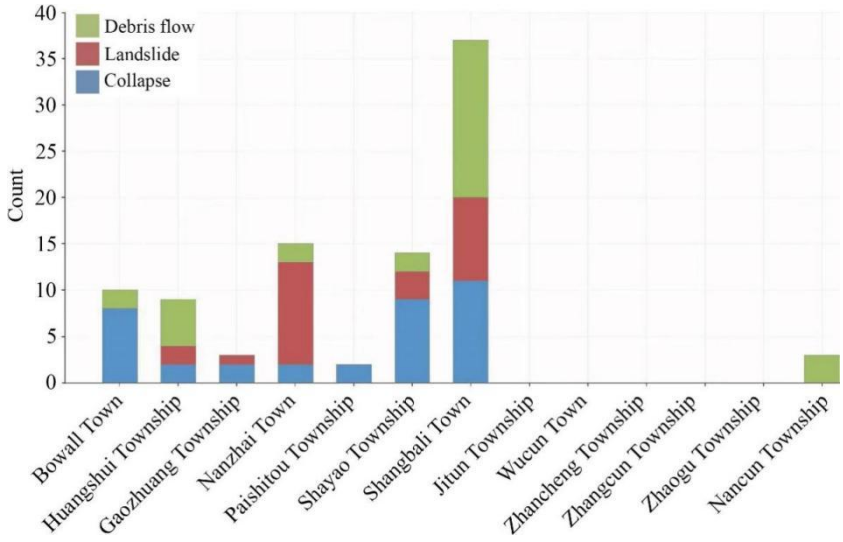

Fig 4. Distribution map of geological hazard sites by township

The results show that the collapse, landslide and debris-flow hazard grades are mainly general to relatively major. Therefore, Huixian City is classified into two risk levels: relatively major and general.

3.1.2. Relationship between geological hazards and rainfall

Huixian City lies in the mid-latitudes and has a typical continental monsoon climate, characterized by warm and humid conditions. Precipitation is jointly affected by warm/cold air masses, solar radiation, topography/geomorphology and atmospheric moisture, resulting in marked spatiotemporal variability. Temporally, interannual variability is large: the mean annual rainfall reaches about 670 mm, the maximum is 1,089 mm, and the range is as high as 803.6 mm. Rainfall is distributed very unevenly throughout the year and is mainly concentrated in the flood season (June–August), while winter rainfall is scarce, with almost no rainfall in January and December. Over the long term (1965–2015), the mean annual rainfall is 577.8 mm, decreasing by about 1.3 mm per decade; the mean annual number of rainy days is 73.6, decreasing by 0.7 day per year. Seasonal differences are obvious: summer contributes the largest share but shows a decreasing trend; winter rainfall intensity increases with more rainy days; spring and autumn total rainfall increases, but daily rainfall tends to decrease. Spatially, mountains and elevation strongly influence rainfall, producing distinct regional patterns: the northwestern mountains and the Nancun Basin receive the most precipitation (mean annual 741.59 mm), the mountainous area averages 619.28 mm, while the plain averages only 598.82 mm, generally decreasing from mountains to plains.

Consistent with the precipitation pattern, the occurrence of geological hazards in Huixian City matches well with the rainfall distribution during June–September. Data for 2003–2005 (Table 2) show that 59, 108 and 23 collapse–landslide–debris-flow events occurred, respectively; among them, 30, 63 and 14 were triggered by heavy rainfall. The proportion of rainfall-triggered events increased year by year, from 50% in 2003 to 58% in 2004 and 61% in 2005, indicating that heavy rainfall is a key triggering factor[14]. In addition, precipitation affects rocks through multiple processes. Physically, infiltration reduces friction along discontinuities, lowers cohesion and friction resistance, and enhances connectivity among rock particles. Chemically, water induces ion exchange, dissolution, corrosion, hydration and hydrolysis, altering mineral composition and mechanical behavior. Mechanically, increased water content and unit weight soften rock–soil masses, reduce shear strength and anti-sliding resistance, and can ultimately trigger landslides. Under natural conditions, collapses, landslides and debris flows may transform into one another. During heavy rainfall, continuous accumulation of collapsed debris may induce landslides with abundant rockfall. Under special terrain and climate conditions, these processes may further evolve into debris flows, posing severe threats to ecosystems and public safety.

Table 2 Statistics of slope geological hazards in Huixian (2003–2005)

Year	Landslide–avalanche–debris-flow disaster count(1)	Rainfall-induced landslide-debris flow disaster count(2)	(2)/(1) (%)
2003	59	30	50
2004	108	63	58
2005	23	14	61

3.2. Analysis of soil–water characteristic tests

Mineral composition, pore structure and water content are key factors controlling the shape of the soil–water characteristic curve (SWCC). This study focuses on the relationship between matric suction and water content during drying (desorption) and wetting (absorption). Because SWCC varies most significantly within 0–400 kPa, a ceramic pressure-plate method was used to measure SWCC in this range. To reduce human errors in specimen preparation and the influence of organic matter,

parallel specimens were used for the drying branch: multiple specimens were placed simultaneously under each pressure level, outliers with high dispersion were removed, and the mean water content at each pressure level was taken as valid data. For the wetting branch, four specimens were used due to instrument volume limitations, and the mean water content at each pressure level was also used. Finally, drying and wetting curves were obtained with matric suction on the x-axis and water content on the y-axis (Figs. 5 and 6).

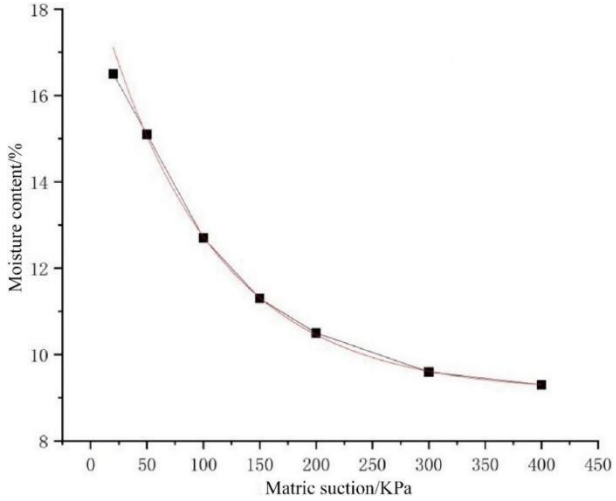

Fig 5. Drying (desorption) branch of the SWCC

The test data were fitted in Origin software. An exponential function was used to describe the SWCC. The expressions for the drying and wetting branches are respectively:

$$\omega = a * e^{\frac{-u}{b}} + c \tag{5}$$

where, ω is the water content (%); u is matric suction (kPa); a,b, and c are fitting parameters, with $a = 9.756$, $b = 100.867$, $c = 9.115$. The correlation coefficient is $R^2 = 0.99984$.

$$\omega = a * e^{\frac{-u}{b}} + c \tag{6}$$

where, $a = 6.594$, $b = 110.04$, $c = 8.589$. The correlation coefficient is $R^2 = 0.99983$.

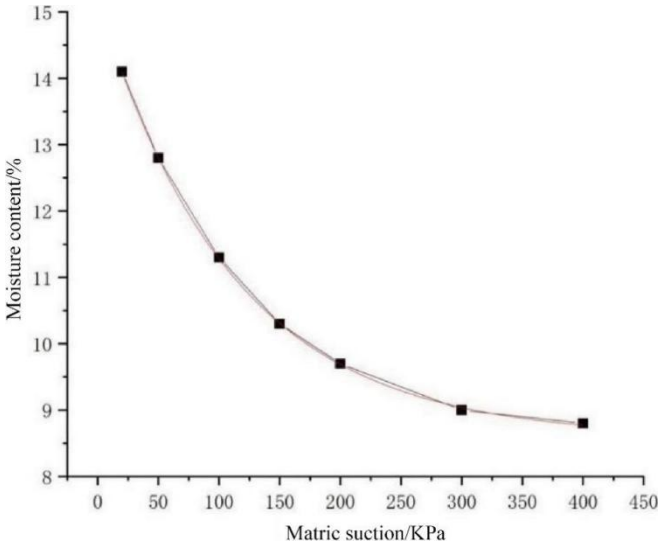

Fig 6. Wetting (absorption) branch of the SWCC

The sample correlation coefficient is expressed by R or R^2. For example, if $r > 0$, the variables are positively correlated; $r = 1$ indicates perfect positive correlation. If $r < 0$, the variables are negatively correlated; $r = -1$ indicates perfect negative correlation. When the correlation is perfect, all points lie

on a straight regression line. The smaller the absolute value, the more dispersed the points; conversely, the closer the value is to 1, the more concentrated the points. A value of 0 indicates no correlation. When the absolute value is not less than 0.75, the variables are strongly correlated. In this study, the correlation coefficients are close to 1, indicating that the established equations can well reflect the variation of SWCC.

A comprehensive analysis of the complete SWCC (Fig. 7) reveals the following mechanisms[12]: (1) pronounced hysteresis. During drying, matric suction increases as water content decreases, whereas during wetting the opposite trend occurs. However, the two paths differ markedly, forming a clear hysteresis loop; the difference is greatest at low suction (near-saturation zone), and the two curves gradually converge as suction increases (low water-content zone). (2) sensitivity zoning. In the near-saturation zone (low suction), water content is highly sensitive to suction changes—small suction fluctuations can cause large water-content changes. In contrast, in the low-saturation zone (high suction), water content changes more gently with suction. (3) stress-path dependence. The mechanical behavior of the soil depends strongly on whether it experiences a wetting or drying path; changes in water content alter matric suction and directly affect soil strength.

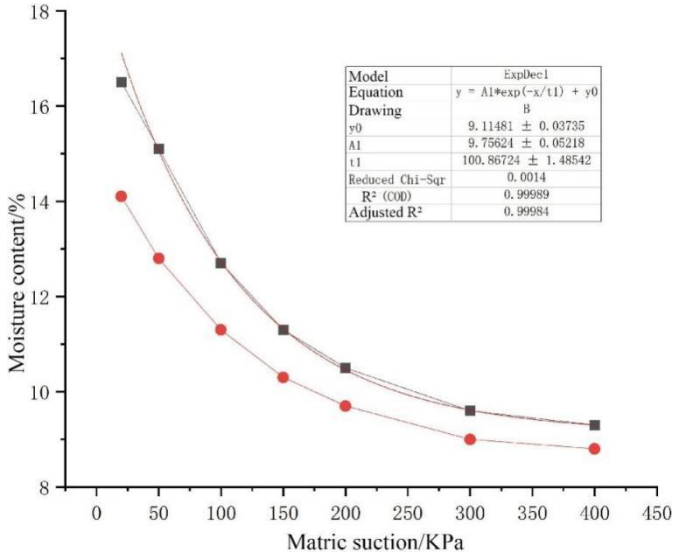

Fig 7. Complete soil–water characteristic curve (SWCC)

These features provide experimental evidence for explaining strength degradation when slope soils transition from unsaturated to saturated during rainfall infiltration.

3.3. Effect of water content on the shear strength of silty clay

To investigate the mechanism by which rainfall infiltration affects soil strength, the dry density was kept constant at 1.60 g/cm³, and four water-content levels (21%, 23%, 25% and 28%) were tested using single-box direct shear tests. Table 3 summarizes the results. The shear strength of silty clay shows a significant nonlinear relationship with water content, exhibiting a parabolic trend of "increase first, then decrease" (Fig. 8).

Table 3 Test data for pulverised clay

Dry density	Moisture content	Cohesion	Angle of friction
	21%	4.3kPa	26.1°
	23%	7.2kPa	25.7°
	25%	11.4 kPa	25.1°
$1.60_{g/cm^3}$	28%	6.7kPa	25.8°

Specifically, when water content increased from 21% to 25%, cohesion rose from 4.3 kPa to 11.4 kPa (peak). When water content further increased to 28%, cohesion dropped sharply to 6.7 kPa.

This indicates an optimum water content of about 25%, at which the soil is denser and interparticle bonding is strongest; beyond this threshold, strength degrades markedly.

Further analysis shows that cohesion and water content follow a quadratic parabolic relationship. By fitting the data, the relationship is obtained as:

$$c=aw^t+bw+d \tag{7}$$

Parameters: $_a$= −3868.1,$_t$ = 2,$_b$=1940.4, $_d$= −233.1. The correlation coefficient is R^2 = 0.8651, greater than 0.75, indicating a strong correlation.

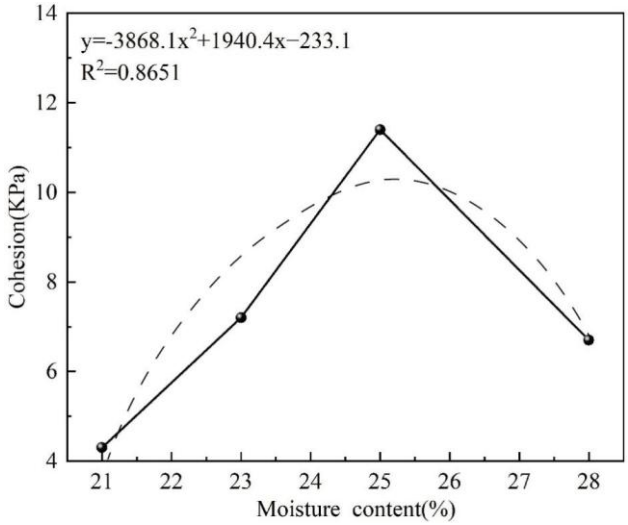

Fig 8. Relationship between cohesion and water content for silty clay

This pattern originates from the dynamic evolution of the bound-water film. Before the optimum water content, a moderate amount of water enhances interparticle bonding via capillary effects. After the threshold is exceeded, an overly thick water film produces a lubrication effect, weakening interparticle friction resistance and causing cohesion to decline. In contrast, the internal friction angle is only weakly influenced by water content (Fig. 9), fluctuating within a narrow range of 25.1°–26.1° from 21% to 28%, suggesting it is mainly controlled by inherent properties such as mineral composition, gradation and density.

From the physical perspective, strength degradation of silty clay is mainly governed by cohesion. At low water content (<25%), the bound-water film is thin and the pore-air pressure maintains relatively high matric suction; compaction during construction makes the soil denser. When rainfall increases the water content beyond the optimum (>25%) toward the liquid limit, the thickened water film not only reduces matric suction, but also generates a “water-wedge” effect through pore-water pressure. The reduction in effective stress causes interparticle bonding to collapse. This is consistent with the SWCC feature that “water content is highly sensitive at low suction,” and explains a key threshold for rainfall-triggered failures: once the slope water content exceeds the optimum (transitioning from about the natural 22.3% toward 25%), shear strength drops rapidly along the descending branch of the parabola, triggering instability.

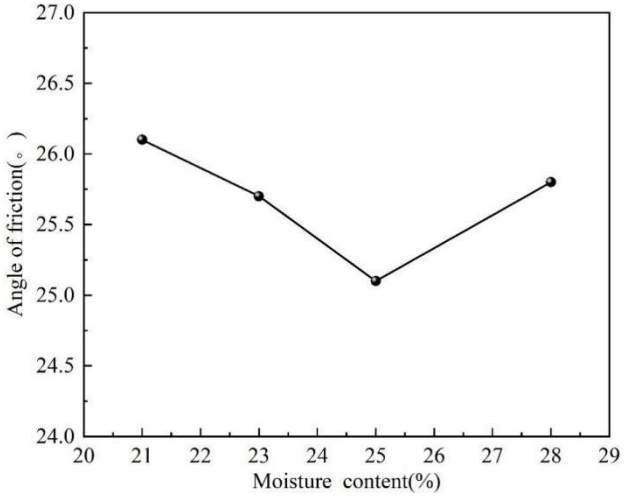

Fig 9. Relationship between friction angle and water content for silty clay

4. CONCLUSION

Based on the geological environmental analysis of Huixian City, laboratory tests on soil physical–mechanical properties, and the rainfall–hazard relationship, this study reveals the main characteristics and triggering mechanism of heavy-rainfall-induced geological hazards. The main conclusions are as follows:

(1) Rainfall-induced geological hazards in Huixian City are mainly collapses/rockfalls, landslides, and debris flows, predominantly of small to medium scale. Their occurrence is strongly correlated with rainfall and mainly concentrated in the flood season (June–October).

(2) The SWCC tests established the quantitative relationship between matric suction and water content of unsaturated silty clay, providing a basis for analyzing its hydro-mechanical behavior under rainfall infiltration.

(3) The shear strength of silty clay shows a nonlinear trend with increasing water content, first increasing and then decreasing. Cohesion reaches its maximum near the optimum water content and then declines rapidly, indicating that water content is a key factor affecting soil stability.

(4) Compared with the internal friction angle, cohesion is much more sensitive to changes in water content and plays a dominant role in controlling slope stability.

(5) The triggering mechanism of heavy-rainfall-induced geological hazards can be summarized as: rainfall infiltration increases water content, reduces matric suction, weakens cohesion and shear strength, and finally induces slope instability. When water content exceeds the optimum level and continues to increase, the risk of collapse and landslide rises significantly.

DECLARATION OF COMPETING INTEREST

The authors declare that they have no known competing financial interests or personal relationships that could have appeared to influence the work reported in this paper.

DATA AVAILABILITY

Data will be made available on request.

ACKNOWLEDGMENTS

This work was supported by the China Postdoctoral Science Foundation (Grant No. 2021M701097), the National Natural Science Foundation of China (Grant No. 42402184), and the Open Project of Henan Key Laboratory of Safety Technology for Water Conservancy Project (Grant No. HNAZ202505).

REFERENCES

[1] YAN Dan, SONG Peng-fei, XIAN Feng. Study on geological environment and geo-hazards status in Huixian City, Henan Province[J]. Xinjiang Nonferrous Metals, 2021, 44(05): 16-19. (in Chinese)

[2] T. M B, S. P, M. R et al. Rainfall thresholds for the possible occurrence of landslides in Italy[J]. Natural Hazards and Earth System Science, 2010, 10(107): 447-458.

[3] Rahardjo H, Li W X, Toll G D et al. The effect of antecedent rainfall on slope stability[J]. Geotechnical and geological engineering,2001, 19(3-4): 371-399.

[4] Segoni S, Piciullo L, Gariano L S. A review of the recent literature on rainfall thresholds for landslide occurrence[J]. Landslides, 2018, 15(8): 1483-1501.

[5] Glade T. Establishing the frequency and magnitude of landslide-triggering rainstorm events in New Zealand[J]. Environmental Geology, 1998, 35(2): 160-174.

[6] Guzzetti F, Peruccacci S, Rossi M, et al. Rainfall thresholds for the initiation of landslides in central and southern Europe [J]. Meteorology and Atmospheric Physics,2007, 98(3-4): 239-267.

[7] Tsaparas I, Rahardjo H, Toll D et al. Controlling parameters for rainfall-induced landslides[J]. Computers and Geotechnics, 2002, 29(1): 1-27.

[8] Dai F, Lee C, Ngai Y. Landslide risk assessment and management: an overview[J]. Engineering Geology, 2002, 64(1): 65-87.

[9] Qi S, Xu Q, Lan H et al. Spatial distribution analysis of landslides triggered by 2008.5. 12 Wenchuan Earthquake, China[J]. Engineering geology, 2010, 116(1-2): 95-108.

[10] Zhu Z, Gan S, Yuan X et al. Landslide susceptibility mapping with integrated SBAS-InSAR technique: a case study of Dongchuan District, Yunnan (China)[J]. Sensors, 2022, 22(15): 5587.

[11] Fredlund D G, Xing A. Equations for the soil-water characteristic curve[J]. Canadian geotechnical journal, 1994, 31(4): 521-532.

[12] Ng, Charles WW, and Y. W. Pang. Influence of stress state on soil-water characteristics and slope stability[J]. Journal of geotechnical and geoenvironmental engineering 126.2 (2000): 157-166.

[13] Li A G, Yue Z Q, Tham L G, et al. Field-monitored variations of soil moisture and matric suction in a saprolite slope[J]. Canadian Geotechnical Journal, 2005, 42(1): 13-26.

[14] Tu X, Kwong A, Dai F et al. Field monitoring of rainfall infiltration in a loess slope and analysis of failure mechanism of rainfall-induced landslides[J]. Engineering Geology, 2008, 105(1-2): 134-150.

[15] Zhang L L, Zhang J, Zhang M L et al. Stability analysis of rainfall-induced slope failure: a review[J]. Proceedings of the Institution of Civil Engineers - Geotechnical Engineering, 2011, 164(5): 299-316.